Available online at www.sciencedirect.com
ScienceDirect
Cement and Concrete Research 36 (2006) 1908–1914
Cement and Concrete Research

Failure mechanisms and tensile relaxation of bonded concrete overlays subjected to differential shrinkage

H. Beushausen *, M.G. Alexander

University of Cape Town, Department of Civil Engineering, Private Bag, Rondebosch, 7701, South Africa

Received 18 October 2005; accepted 29 May 2006

Abstract

Restraint of shrinkage deformations is the main factor influencing the serviceability and durability of bonded concrete overlays. Failure mechanisms associated with differential shrinkage stresses are cracking and debonding. Tensile overlay relaxation may release a considerable amount of the imposed stresses and is therefore of major importance for the performance of the overlay. Composite specimens were used for the identification of fundamental characteristics of strain development of bonded concrete overlays, with regard to different interface textures and overlay materials. The development of overlay strains and material parameters in relation to the observed mechanisms of overlay failure allowed an estimation of the magnitude of tensile relaxation. A simplified approach to tensile stress relaxation in bonded overlays is introduced.

Keywords: Concrete overlay; Differential shrinkage; Tensile relaxation; Debonding; Cracking

1. Introduction

The bonded concrete overlay technique is particularly suitable for the repair, lining, and retrofitting of concrete structures, roads and pavements. Stresses due to differential volume changes have long been recognised as the main problem for the performance of bonded concrete overlays [1–7]. Direct overlay stresses are caused by the restraint of expansion or contraction parallel to the interface, whereby tensile stresses resulting from restraint contraction are the most critical and can result in extensive cracking.

Regarding the above, differential shrinkage is generally considered to be the most critical influence on the long-term performance of composite members. The mechanisms of shrinkage in concrete members are well known. The effects of differential shrinkage on the performance of bonded overlays have however not been fully clarified. This is mainly due to the large number of influences on differential shrinkage stresses, which are difficult to assess independently and which include time-dependent material characteristics, environmental conditions, structural properties of the system, and the effects of workmanship.

Tensile stress relaxation has also been recognised as one of the most important factors for stress development in overlays subjected to restrained shrinkage [6–12]. However, information on tensile relaxation is limited and to the knowledge of the authors no information on relaxation values directly measured on bonded overlays is discussed in the literature. This paper discusses experiments performed on composite members of realistic dimensions, consisting of substrate concrete beams and different overlay materials. Depending on interface texture and overlay composition, failure was observed as overlay cracking or debonding. The mechanisms of failure in connection with strain measurements allowed an estimation of overlay relaxation characteristics under practical conditions.

2. Background

Bonding a new concrete overlay to an existing substrate results in restraint of differential volume changes between the two composites. The restraint of overlay volume changes results in locked-in strain energy, which, depending on the magnitude of restrained deformation and elastic properties, causes tensile stresses in the overlay and shear stresses at the interface.

* Corresponding author. Fax: +27 21 689 7471.
E-mail address: ICCRRR@eng.uct.ac.za (H. Beushausen).

0008-8846/$ - see front matter © 2006 Elsevier Ltd. All rights reserved.
doi:10.1016/j.cemconres.2006.05.027

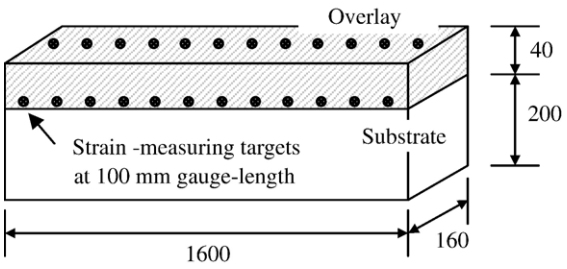

Fig. 1. Schematic of test specimens and application of strain-measuring targets.

The free shrinkage strain ε_{FSS} of most of the common overlay materials is far higher than their tensile strain capacity of 100.10^{-6} to 200.10^{-6} [7]. Restrained shrinkage stresses therefore often exceed tensile overlay strength and cause cracking, which affects the appearance of the member and may impair its durability through the ingress of harmful substances. Another common mechanism of locked-in strain energy release is overlay debonding, which may lead to local delamination and spalling. Debonding is related to cracking as it is commonly initiated at overlay boundaries such as free edges, joints, and cracks [13–15].

Overlay stresses are partly released through tensile relaxation. In absence of detailed information, the estimation of such relaxation is often based on creep strain characteristics. However, the mechanics of overlay relaxation, i.e. the decrease in stress under constant strain, might differ from the mechanisms of tensile creep, which denote the increase in strain under constant stress. An important aspect for the performance of bonded overlays is the time-dependence of visco-elastic mechanisms. In experiments discussed in Ref. [10], it took only 2–3 h to reach the ultimate values of tensile relaxation in specimens subjected to constant strain, irrespective of the stress–strength ratio which ranged from 0% to 60%. Specimens were tested at different ages between 1 and 21 days, with the observation that ultimate relaxation decreases with the age of the member. Similarly, experiments discussed in Ref. [9] showed that the initial stress–strength ratio has no significant influence on tensile relaxation. In the study referred to, relaxation after 100 h was found to be 35–50% of the initial stress. Kordina et al. [16] tested different concrete mixes for tensile relaxation and found that ultimate relaxation values were reached after approximately 2 days. In their tests, relaxation was 50–60% of initial tensile stress. Pigeon et al. [12] tested relaxation of concrete subjected to restrained shrinkage at early ages and found that creep deformations accounted for almost 67% of the free shrinkage value.

For the evaluation of the effects of restrained shrinkage on overlay cracking characteristics, a number of restrained shrinkage tests are available, the two most common types being the “dog-bone” test and the ring test [17]. The mechanisms, advantages and disadvantages of available tests have been documented in detail in the literature [18,19]. Pigeon et al. [12] developed a test equipment for the evaluation of visco-elastic deformations in fully restrained specimens. This equipment has the advantage that it can evaluate the determination of visco-elastic deformations with time, giving a clear indication of actual relaxation values. With these test methods, the relative effects of material variations on induced tensile stresses and cracking potential can be estimated. Restrained shrinkage tests have been used extensively for the prediction of cracking in restrained concrete and mortar specimens. In general they provide a good estimation of the influences of different material properties on the developments of tensile stress and stress relaxation. However, these test methods commonly do not represent the degree of restraint experienced in actual composite members and it appears more practical to resort to tests which provide information which is of physical relevance both in terms of material parameters and the nature of the structural system with respect to the restraint it produces.

3. Experimental research

3.1. Test specimens

For testing shrinkage-induced strain characteristics of composite members, specimens consisting of a substrate concrete beam ($1600 \times 155 \times 200$ mm) with a 40 mm overlay were prepared. Strain-measuring targets were applied on the overlay at 100-mm gauge length both at the interface as close to the substrate as possible, and on top along the centre-line of the overlay (Fig. 1). Strains were measured using an extensometer with a gauge length of 100 mm and a measuring accuracy of 0.001 mm (i.e. 10 microstrain).

The substrate concrete of all specimens was at least 9 months old at the time of overlay placement to make sure that most of its drying shrinkage had taken place. Different substrate surface preparations, and hence different interface textures between substrate and overlay, were selected to study the effects of micro- and macro-roughness and the resulting degree of restraint at the interface. Specimens with smooth substrate surfaces were used to study differential shrinkage of composite members with relatively little mechanical restraint at the interface. Smooth surfaces were cast against steel formwork and, except for surface blow-holes, had a roughness only on microscopic scale. Sandblasting was used to provide an interface with good micro-roughness. Due to the originally

Fig. 2. Notched interface.

Table 1
Substrate and overlay mix proportions and material properties

		Substrate	Overlay 1	Overlay 2
Cement CEM I	[kg/m^3]	350	640	510
Water	[kg/m^3]	175	300	235
19 mm Greywacke	[kg/m^3]	1025	–	–
9 mm Greywacke	[kg/m^3]	–	–	940
Sand, max. 2 mm	[kg/m^3]	875	1300	660
W/*C* ratio	[–]	0.50	0.47	0.46
Slump	[mm]	90	Collapse	80
28-d compr. strength	[MPa]	48.4	50.9	53.3
28-d tensile split strength	[MPa]		2.1	3.0
28-d elastic modulus	[GPa]	28.1	22.1	29.6
28-d ε_{FSS}	[10^{-6}]		540	290

smooth surface of the beams, the sandblasted interfaces had virtually no macro-roughness, i.e. the overall surface texture of the substrate beams was relatively smooth. The average surface roughness of all sandblasted specimens, measured with the Sand-Area Method [20], was 0.7 mm. Substrate members with notched surfaces were prepared to represent interfaces with well-defined macro roughness and minimum of micro roughness (Fig. 2).

Two different overlays with different shrinkage characteristics were tested. Overlay and substrate mix proportions and selected material properties are presented in Table 1. Both Overlay 1 and 2 were applied to substrate members with smooth and sandblasted interfaces. In addition, Overlay 1 was applied to substrate specimens with notched surface textures (Table 2). For Specimens A, 2 beams were prepared per test parameter; for Specimens B, one beam was prepared per test parameter. Test results presented in the following sections are mean values from all measurement locations along the specimens.

Strains measured on the composite specimens were compared to free overlay shrinkage strains, which were measured on specimens with the same cross-sectional dimensions as the overlays (155×40 mm^2). The free-shrinkage specimens were placed next to the respective test specimens to ensure exposure in the same environment. The lower faces of the free-shrinkage specimens were not sealed as the authors believe that completely unsealed specimens best represent the boundary conditions experienced in the actual overlay. The overlay looses moisture to the environment through its exposed surfaces. It however also looses moisture to the substrate, as the latter is commonly relatively dry and consequently tends to absorb water from the overlay. In free shrinkage specimens, this situation could not be simulated by sealing one of the faces.

All specimens were moist cured for a period of 7 days after overlay casting and subsequently exposed to laboratory environment with temperatures and relative humidity ranging from 16 to 21 °C and 55% to 75% RH respectively.

3.2. Test results and observations

3.2.1. General

Specimens A1–A3 showed extensive cracking at early ages. From visual observations and strain measurements on these specimens, characteristics of overlay crack development could be identified. The mechanisms of debonding are discussed using observations and strain readings of Specimen B1. Strain measurements prior and subsequent to the occurrence of overlay failure allowed an estimation of the magnitude of overlay stress relaxation in the above specimens. In addition, Specimen B2 was used for the estimation of tensile relaxation on an uncracked and fully bonded overlay. It must be noted that strain measurements across cracks cannot be used to estimate crack widths. They do however provide useful information on the overall strain behaviour of cracked specimens and can thus be used to analyse stress development and relaxation properties.

The influence that the varying environmental conditions in the laboratory had on strain readings are evident in the free shrinkage strain shown in Figs. 3–9.

3.2.2. Characteristics of overlay cracking

The overlays of Specimens A1–A3 cracked extensively during the first weeks. This was the result of the combined influences of a high rate of shrinkage development at early ages and low tensile strength (compare Table 1). The majority of cracks traversed the entire width and depth of the overlay. Cracks were identified visually using a magnifying glass and were found to occur, independent of interface texture, at relatively regular spacing of 100 to 200 mm.

Strain measurements across the cracks were interpreted in connection with visual observations. Strain values at different cracked locations along the members showed a large scatter of results, indicating that some cracks opened wider than others. To facilitate the analysis of strain measurements, the mean values of all strains measured across the cracks of each specimen are used in the following discussion. The short-term strain development of Specimens A1–A3 is presented in Figs. 3–5. In the current context, "short-term" was defined as the time period ending roughly 30 days after completion of curing. Strains measured across uncracked locations of the specimens are presented as a comparison. Once again, these are the mean values of all locations along the specimens.

The majority of cracks on Specimens A1–A3 appeared between 6 and 10 days after completion of curing. Locations that were going to crack showed lower initial strain, compared to the locations that did not crack. These lesser values were a sign of incipient cracks, indicating that the locations of major cracks were somewhat predestined. Compared to Specimens A1 and A2, Specimens A3 (notched interface) showed different strain characteristics prior to cracking. Cracked locations showed negative strain values (i.e. crack-opening strains) from the beginning of the test period. Cracks were only identified visually after approximately 7 days but the strain values indicate that

Table 2
Overview of test specimens

Specimen	Interface texture	Overlay type
A1	Smooth	1
A2	Sandblasted	1
A3	Notched	1
B1	Smooth	2
B2	Sandblasted	2

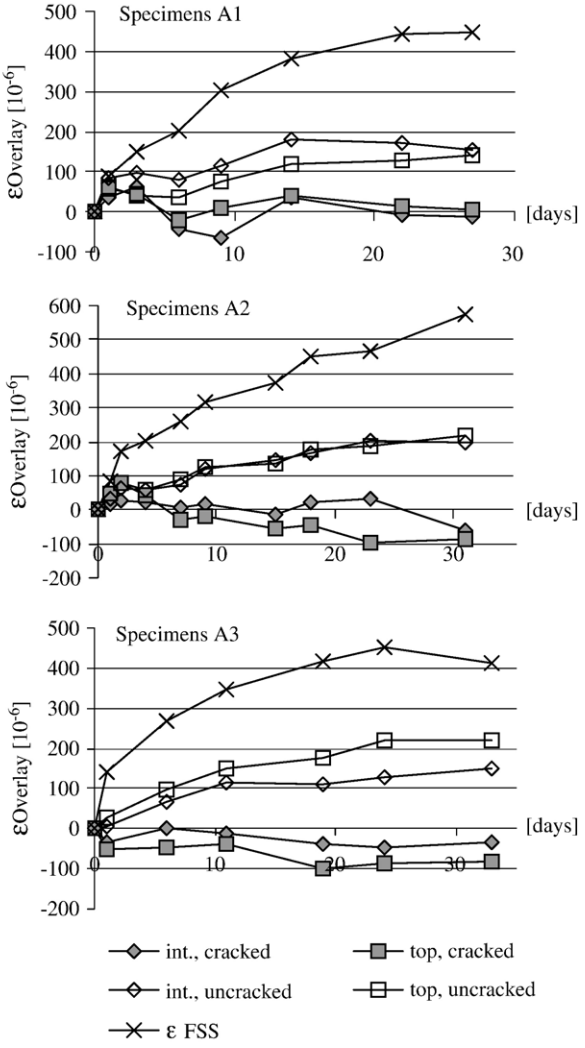

Fig. 3–5. Short-term overlay strain development of Specimens A1-3 at cracked and uncracked locations, and free overlay shrinkage strain.

cracks probably developed earlier, which could have been a result of the high mechanical restraint provided by the notches.

Strain at the cracked locations generally followed a negatively increasing trend, indicating further opening of cracks. However, this increase in negative strain was relatively small. An increase in crack width at the interface would have been connected to local debonding at the cracked locations. The small increase of negative strain values at cracked locations at the interface indicated that major debonding probably did not occur during the test period. This observation was confirmed for long-term behaviour of the specimens as measurements taken over 2 years revealed no further opening of cracks at the interface, despite high continuous shrinkage strain (Figs. 6–8). Over the test period, overlay strains at the interface of all specimens increased towards positive strain values, indicating that crack opening did not occur. Specimens A2 and A3 showed less positive strain across cracks on top of the member, indicating that on top crack widths were larger than at the interface. Actual crack widths were however not measured on the specimens.

The hammer-tapping method, with which debonded areas can be identified, confirmed that the bond was intact at all locations along the members. This is noteworthy especially for the smooth interfaces of Specimens A1, which offered low mechanical restraint of overlay slip. Bond failure, which is sometimes observed in actual composite members next to cracks, can therefore probably be related to the influences of poor interface preparation or cyclic loading due to temperature changes rather than the influences of differential shrinkage.

The strain development of Specimens A1 and A2 clearly indicated the time of overlay cracking, as discussed above. The estimation of overlay relaxation is therefore based on these specimens, using a simple analytical procedure. Overlay strains ε_O and free shrinkage strains ε_{FSS} are compared at the time just before cracking, the difference between the two indicating the magnitude of restrained overlay shrinkage. In absence of relaxation, the magnitude of restrained shrinkage can directly be related to tensile stress, using the elastic modulus of the overlay

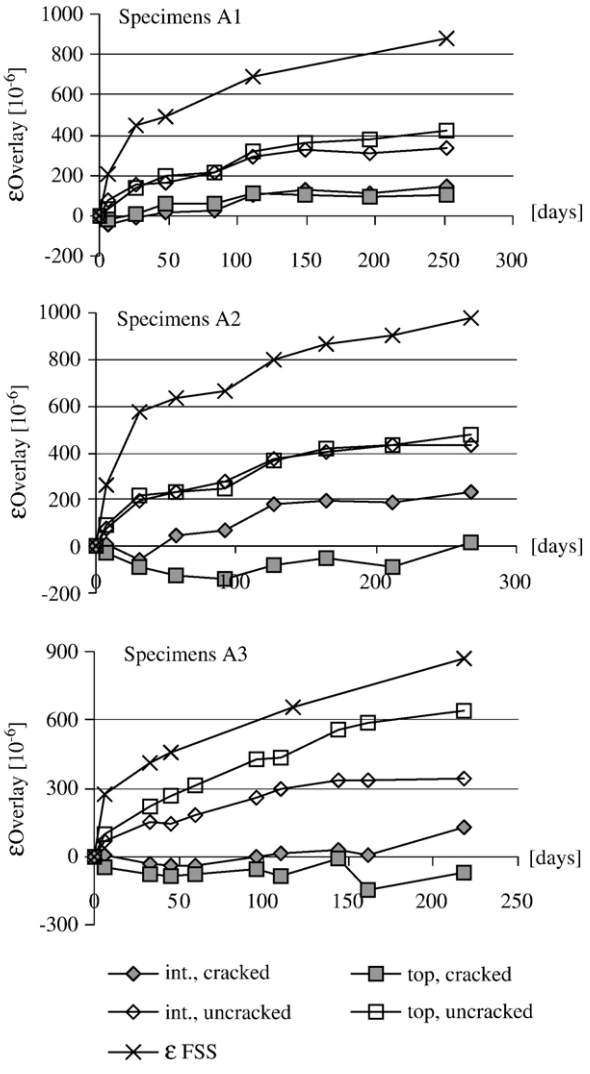

Fig. 6–8. Long-term overlay strain development of Specimens A1-3 at cracked and uncracked locations, and free overlay shrinkage strain.

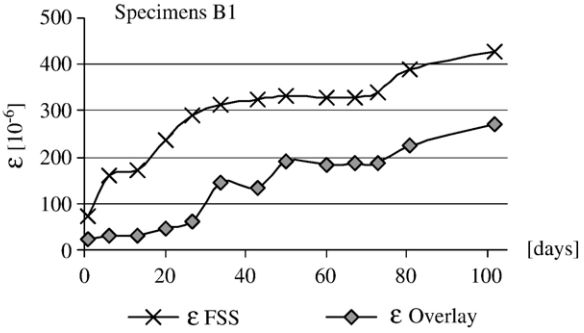

Fig. 9. Specimen B1, overlay strain development and free shrinkage strain.

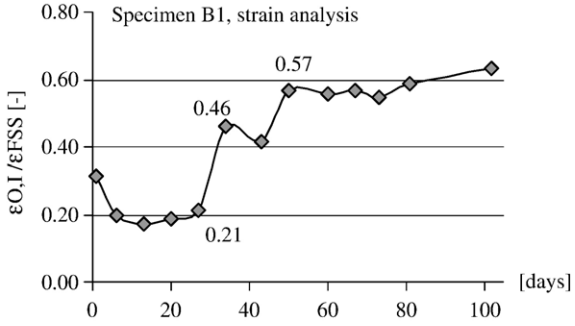

Fig. 10. Specimens B1, ratio between overlay strain at the interface and free shrinkage strain.

E_O. Comparing the computed tensile stress to tensile overlay strength $f_{t,O}$ indicates the magnitude of stress relaxation:

$$\psi_o = \frac{f_{t,O}}{(\varepsilon_{FSS} - \varepsilon_O)E_O} \quad (1)$$

where ψ_O is the relaxation factor of the overlay. Using the above method, the magnitude of tensile stress relaxation for Specimens A1 and A2 was found to be between 40–50% at 7 days.

3.2.3. Characteristics of overlay debonding

The overlay of Specimen B1 debonded from the substrate after approximately 4 weeks. No cracks developed in the overlay which remained intact, and debonding was thus the sole mechanism of stress release. Debonding was observed visually as the overlay had clearly separated from the substrate over approximately 80% of the member length. Debonding started on one end only while the other end remained bonded to the substrate over the whole test period. Overlay strains at the interface, in comparison to free overlay shrinkage strains, are presented in Fig. 9.

During approximately the first 2 weeks, overlay strain developed at a fairly slow rate. In Fig. 9, debonding is indicated through the sudden jump of overlay strain after approximately 4 weeks. Subsequent to the onset of debonding, overlay strain developed at a faster rate than free shrinkage strain. Thereafter, overlay and free shrinkage strains increased at virtually the same rates, indicating that the overlay was now able to shrink freely. The step in the overlay strain curve between days 28 and 42 suggests that the bond was destroyed in stages, confirming observations discussed in Ref. [14].

To analyse Specimen B1 in terms of overlay relaxation, overlay strains are compared to free shrinkage strains (Fig. 10). The low ratio between overlay shrinkage and free shrinkage of approximately 0.2 during the first 4 weeks indicates high initial restraint. The onset of debonding led to a sudden increase in the ratio to a value of 0.47, and after approximately 7 weeks, when debonding was completed, the ratio reached a value of 0.57. The difference in overlay strain between the onset and completion of debonding denotes the elastic component of restrained shrinkage, i.e. the component that could be recovered after the restraining action was eliminated. The inelastic component of restrained shrinkage, i.e. the component that could not be recovered after debonding, is expressed through the difference between free shrinkage strain and overlay strain at the completion of debonding. This strain difference corresponds to the stress and strain released. In that respect, the ratio between overlay shrinkage and free shrinkage of 0.57 at the completion of debonding corresponds to the relaxation factor ψ. Therefore, during the first 7 weeks, overlay relaxation led to a reduction of restrained shrinkage stress of approximately 43%.

3.2.4. Tensile relaxation in fully bonded, uncracked overlays

Specimens B2 showed no failure during the test period as cracks and debonding were prevented through the relatively low shrinkage strains and the good mechanical bond at the interface respectively. The numerical difference between overlay strain and free shrinkage indicates the rate of tensile stress development (Fig. 11), which in absence of cracking can be compared to tensile strength in order to estimate the magnitude of stress relaxation:

$$\psi_o \leq \frac{f_{t,O}}{(\varepsilon_{FSS} - \varepsilon_O)E_O} \quad (2)$$

Based on the above, the tensile relaxation factor ψ_O in Specimen B2 was found to be no more than 0.71, 0.50, and 0.43 (corresponding to at least 29%, 50%, and 57% stress relaxation) at ages of 28, 50 and 100 days respectively. These values represent the minimum relaxation the specimen experienced as the actual value can only be identified at the moment of overlay failure. The relatively high relaxation values explain the absence of cracks during the test period, during which the imposed tensile strain, i.e. the restrained compressive strain, clearly exceeded the tensile strain capacity which is commonly

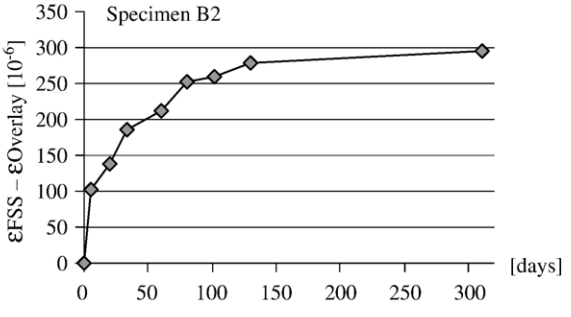

Fig. 11. Specimen B2, development of restrained overlay strain.

assumed to be in the region of 100–200.10^{-6} for normal concretes.

3.2.5. Discussion of the experimental research

It is interesting to note that the degree of mechanical restraint at the interface, defined by the interface texture, had no influence on the cracking behaviour of the specimens. On all specimens that cracked, cracks occurred during the first few days at regular spacings of 100–150 mm. Similarly, long-term strains at uncracked locations were very similar for all specimens, irrespective of the interface texture. The degree of overlay restraint in these specimens could therefore not be related to macro-mechanical interaction at the interface.

The influence of the interface texture was however revealed through overlay debonding in Specimen B1 (smooth surface). Macro-mechanical bond at the interface, in Specimen B2 provided by the sandblasted substrate surface, proved to be important for Overlay 2, which resisted cracking through sufficient tensile strength and stress relaxation. This leads to the conclusion that for overlays that resist cracking macro-mechanical bond at the interface is important to prevent the release of locked-in restraint energy through debonding. On cracked specimens, no debonding was observed, irrespective of the low interface roughness of Specimens A1 and high ongoing shrinkage strains. Similarly, no cracking was observed on the debonded overlay of Specimen B1. It appears that overlay failure resulting from restrained shrinkage is manifested in a single failure mechanism, i.e., depending on material parameters and interface texture, in either cracking or debonding. Combinations of the two mechanisms in actual structures is probably a result mainly of poor substrate surface preparation (e.g. unclean interfaces) or cyclic stresses resulting from thermal influences.

The estimation of overlay relaxation in cracked Specimens A indicated a relatively large amount of relaxation in the first week after completion of curing. For the overlays under investigation, relaxation could be estimated to be approximately 45%. Relaxation factors of similar magnitude were computed for Specimens B. In general, relaxation reduced tensile stress by approximately 40–50%, which is of the same order of magnitude as that reported in the literature [9,10,16]. Pigeon et al. [12] measured relaxation values of fully restrained specimens in the order of 67%, which is considerably higher that the values reported in this study. A general comparison of relaxation values obtained with different concrete mixes and test equipments is problematic. However, results reported in the literature and presented in this study all support the assumption that relaxation is a major mechanism for stress development of concrete specimens under restrained deformation.

4. Designing bonded overlays allowing for tensile relaxation

An important aspect in the design of bonded concrete overlays is that shrinkage is not completely restrained. The degree of restraint and hence the magnitude of actual overlay strain depends on the structural system, i.e. the dimensions and elastic properties of substrate and overlay. Assuming full bond, the substrate will undergo the same deformation at the interface as the overlay, corresponding to its imposed compressive stress, which results in substrate creep deformations and hence further release of tensile stress in the overlay. The total release of tensile overlay stresses is therefore a combination of different components, most important of which are elastic strains resulting from the interaction between substrate and overlay, substrate creep strains, and overlay relaxation.

The influences of overlay relaxation on strains and stresses in the composite member are complex and difficult to assess. Since overlay relaxation is not directly coupled with a reduction in overlay strain, the substrate still experiences the same strain and hence the same stress as at the time of loading. This leads to a redistribution of forces in the member since tension and compression must be in equilibrium. Overlay relaxation influences overlay strains therefore indirectly through the reduction in the actual shrinkage force acting on the composite section and hence through the redistribution of stresses.

The experimental results indicate that a large amount of overlay relaxation occurs at early ages. This observation is supported by the literature as discussed in Section 2. During a certain time period, the relaxation of stresses that have existed at the beginning of that time period develops much faster compared to the build-up of additional stresses during this period. For practical analysis, full relaxation can thus be assumed to occur simultaneously with stress initiation. In estimating tensile overlay stresses, the stress-producing shrinkage strain $\varepsilon_{\sigma(\mathrm{FSS})}$ can thus be adjusted by the time-dependent overlay relaxation factor $\psi_{\mathrm{O}}(t, t_0)$:

$$\varepsilon_{\sigma(\mathrm{FSS})} = \psi_{\mathrm{O}}(t, t_0) \cdot \varepsilon_{\mathrm{FSS}} \tag{3}$$

This approach is based on the assumption that overlay relaxation is of equal importance for tensile stress development as overlay shrinkage. Tensile overlay stresses increase proportionally with increasing shrinkage and decreasing relaxation. Considering that relaxation, next to tensile strength, is the main safety factor for the performance of bonded overlays subjected to restrained shrinkage, this assumption seems appropriate and permits the design of overlay materials accordingly.

The relaxation factor $\psi_{\mathrm{O}}(t, t_0)$ accounts for the total relaxation of incremental stresses from the time of first loading t_0. The relaxation at different time increments depends on the age of the overlay since concrete members have less relaxation when loaded at later ages. The relaxation factor at any given age can be estimated through the time-dependent relaxation function $\Psi(t, t_0)$. For practical application in the case of bonded overlays, the relaxation factor $\psi_{\mathrm{O}}(t, t_0)$ at any time can be estimated to be:

$$\psi_{\mathrm{O}}(t, t_0) = \left(\sum_{t_i=0}^{t} \left(\varepsilon_{\mathrm{FSS}}(t_i) - \varepsilon_{\mathrm{FSS}}(t_i - 1) \right) \cdot \Psi_{\mathrm{O}}(t_i, t_{i-1}) \right) \cdot \frac{1}{\varepsilon_{\mathrm{FSS}}(t)} \tag{4}$$

Relaxation functions $\Psi(t, t_0)$ for tensile creep were introduced in Refs. [9] and [10]. However, further research is

necessary to obtain information on relaxation functions of common overlay materials under practical stress conditions. Due to the complexity of the mechanisms of relaxation in restrained concrete members it appears appropriate to estimate relaxation factors with common restrained shrinkage test methods discussed earlier (e.g. dog-bone test and ring test). However, it should be kept in mind that these test methods do not represent the degree of restraint encountered in real structures. Further research is necessary to link results obtained from common restrained shrinkage test methods to the behaviour of restrained overlays in actual structures.

5. Conclusions

(1) The mode of overlay failure resulting from restrained shrinkage is either cracking or debonding. Combined modes of failure were not observed on the test specimens. In practice, combined modes of overlay failure are probably a result of cyclic temperature stresses, poor workmanship, or structural loads.
(2) Overlay cracking occurs independent from the macro-mechanical restraint provided by the interface texture. The substrate surface texture has no influence on crack resistance as long as the overlay is fully bonded to the substrate.
(3) Low macro-mechanical restraint (i.e. smooth substrate surface textures) at the interface can result in complete debonding if overlay stresses are not released through cracking.
(4) Tensile relaxation in bonded concrete overlays occurs shortly after stress initiation and therefore much faster than the rate of stress increase resulting from continuous overlay shrinkage. To facilitate the prediction of overlay stresses, relaxation can therefore assumed to occur simultaneously with stress initiation. Following this assumption, tensile overlay stress decreases proportionally with increasing overlay relaxation.
(5) Relaxation was found to release approximately 40–50% of tensile overlay stress, indicating its major importance for the serviceability of bonded concrete overlays.
(6) Further research is necessary to obtain information on relaxation properties of common overlay materials under practical conditions.

References

[1] P.H. Emmons, A.M Vaysburd, J.E. McDonald, R.W. Poston, K.E. Kesner, Selecting durable repair materials: performance criteria, Concrete International (2000 (March)) 38–45.
[2] J.L. Granju, 193-RLS RILEM TC Bonded cement-based material overlays for the repair, the lining or the strengthening of slabs or pavements. State of the Art report (draft), France, August 2005.
[3] A.M. Vaysburd, P.H. Emmons, N.P. Mailvaganam, J.E. McDonald, B. Bissonette, Concrete repair technology — a revised approach is needed, Concrete International (2004 (January)) 59–65.
[4] N.K. Emberson, G.C. Mays, Significance of property mismatch in the patch repair of structural concrete: Part 1. Properties of repair systems, Magazine of Concrete Research 42 (152) (1990 (Sept.)) 147–160.
[5] E. Denarié, J. Silfwerbrand, Structural behaviour of bonded concrete overlays. Proceedings, International RILEM Workshop on 'Bonded Concrete Overlays', June 7–8 2004, Stockholm, Sweden, 37–45.
[6] M. Pigeon, B. Bissonette, Bonded concrete repairs— tensile creep and cracking potential, Concrete International (1999 (November)) 31–35.
[7] M. Pigeon, F. Saucier, Durability of repaired concrete structures. Proceedings, International Symposium on Advances in Concrete Technology, Athens, 11–12 May, October 1992, pp. 741–773.
[8] B. Bissonette, M. Pigeon, Tensile creep at early ages of ordinary, silica fume and fiber reinforced concretes, Cement and Concrete Research 25 (5) (1995) 1075–1085.
[9] A. Gutsch, F.S. Rostásy, Young concrete under high tensile stresses— creep relaxation and cracking, in: R. Springenschmidt (Ed.), Proceedings: RILEM Symposium 'Thermal Cracking in Concrete at Early Ages', Chapman & Hall, London, 1995, pp. 111–116.
[10] H. Horimoto, W. Koyanagi, Estimation of stress relaxation in concrete at early ages, in: R. Springenschmidt (Ed.), Proceedings: RILEM Symposium 'Thermal Cracking in Concrete at Early Ages', Chapman & Hall, London, 1995, pp. 95–102.
[11] J. Walraven, H. Shkoukani, Kriechen und Relaxation des Betons bei Temperatur-Zwangsbeanspruchung, Beton- und Stahlbetonbau 88 (1993) 10–15 (Germany, Heft 1).
[12] M. Pigeon, G. Toma, A. Delagrave, B. Bissonnrttr, J. Marchand, J.C. Prince, Equipment for the analysis of the behaviour of concrete under restrained shrinkage at early ages, Magazine of Concrete Research 52 (4) (2000 (Aug.)) 297–302.
[13] J.L. Granju, Thin bonded overlays — about the role of fibre reinforcement on the limitation of their debonding, Advanced Cement Based Materials 4 (1996) 21–27.
[14] P. Carter, S. Gurjar, J. Wong, Debonding of highway bridge deck overlays, Concrete International (2002 (July)) 51–58.
[15] J. Silfwerbrand, Stresses and strains in composite concrete beams subjected to differential shrinkage, ACI Structural Journal 94 (4) (1997 (July–August)).
[16] K. Kordina, L. Schubert, U. Troitzsch, Kriechen von Beton unter Zugbeanspruchung, Deutscher Ausschuss für Stahlbeton, Heft 498, Beuth Verlag, Berlin, Germany, 2000.
[17] ASTM International. Standard test method for determining age at cracking and induced tensile stress characteristics of mortar and concrete under restrained shrinkage. Designation C 1581-04. August 2004, USA.
[18] H. Emmons, A.M. Vaysburd, Performance criteria for concrete repair material, phase 1. Technical Report REMR-CS-47, US Army Corps of Engineers, April 1995.
[19] A. Bentur, Early-age shrinkage and cracking in cementitious systems, Concrete Science and Engineering 3 (2001 (March)) 3–12.
[20] N. Kaufmann, Das Sandflächenverfahren, Strassenbau-Technik 24 (3) (1971) 31–50 (Germany).